



Influence of SiC Nano Particles on Microhardness and Corrosion Resistance of Electroless Ni–P Coatings

Vinod Babu Chintada¹ · Ramji Koonaa²

Received: 6 August 2018 / Revised: 5 September 2018 / Accepted: 12 September 2018 / Published online: 17 September 2018
© Springer Nature Switzerland AG 2018

Abstract

Silicon carbide nanoparticles were co-deposited in Ni–P matrix to form Ni–P–SiC composite coating on the mild steel substrate by using electroless coating technique. In the present study, the effect of SiC nanoparticles concentration and heat treatment temperature on microhardness and corrosion resistance of the Ni–P–SiC coating was investigated. The microhardness and corrosion resistance of the coating was further analyzed through the experiments. X-ray diffraction and scanning electron microscope attached with energy dispersive spectroscopy were used to analyze phase structure, morphology, and elemental composition of the coating. Results confirm that incorporation of SiC nanoparticles into the coating greatly influences the microhardness and corrosion resistance of the coating. The phase change from amorphous Ni to crystalline nickel and nickel phosphide at 400 °C further improves the microhardness and corrosion resistance of the composite coating.

Keywords Electroless coating · Heat treatment · Corrosion · Microhardness

1 Introduction

Electroless Ni is an autocatalytic coating, which means coating formed from the solution on the substrate without electricity. Controlled chemical reduction of Ni ions on a catalytic surface develops the electroless Ni coating [1, 2]. By using this method, substrate was coated uniformly on both (inside and outside) the sides until there was uniform solution flow. Physical vapor deposition (PVP), chemical vapor deposition, thermal spraying, and electrolytic coating cannot achieve uniform thickness across part geometry. The electroless coatings can be classified into three main groups based on phosphorus content: low phosphorus (1–4 wt% P), medium phosphorus (4–10 wt% P), and high phosphorus (> 10.5 wt% P) [3, 4]. The electroless coatings can be deposited on cast iron, carbon steel, stainless steel, aluminum, and magnesium alloys [5, 6]. Usually, the physical and mechanical properties are further improved by composite coatings

formed by embedding the hard ceramic particles such as Al₂O₃, SiC, TiO₂, WC, Si₃N₄, PTFE, MoS₂, diamond, and graphite into the Ni–P matrix [7–9]. Hard particles such as Al₂O₃, SiC, TiO₂, WC, Si₃N₄, diamond used to improve the hardness and to reduce friction PTFE, MoS₂, and graphite particles are used in micro and nano level [10]. S. Afroukhteh found the addition of small amount of Al₂O₃ nanoparticle does not affect much the corrosion potential of the Ni–P coating. The lower porosity of the coating observed at a higher deposition of the Al₂O₃ results in higher corrosion resistance of the Ni–P composite coating [11]. S.A. Abdel found the Ni–P–Al₂O₃ coating increases the corrosion resistance of the copper substrate up to the 70 g/L concentration of Al₂O₃ particles in the bath; beyond this limit decreases the corrosion resistance of the coating due to agglomeration of nanoparticles [12]. S. Karthikeyan found the Ni–P coating hardness increases by embedding the nano Al₂O₃ into the Ni–P matrix. He also confirms the formation of the metal oxide layer during the wear test improves the wear resistance of the Ni–P–nano Al₂O₃ coating on mild steel substrate [13]. C.J. Lin found that size of the SiC particles greatly influence the properties of the composite coating. The coating formed in the presence of SiC nanoparticles offers a smooth surface with good corrosion resistance in 3.5% NaCl solution because a homogeneous distribution of SiC nanoparticles reduces the pores present the coating

✉ Vinod Babu Chintada
vinodbabu.chintada@gmail.com

¹ Department of Mechanical Engineering, GMR Institute of Technology, Rajam, Andhrapradesh 532127, India

² Department of Mechanical Engineering, Andhra University College of Engineering, Andhra University, Visakhapatnam, Andhrapradesh, India

[14]. Lloyd Ploof confirms that the boron nitride-reinforced Ni–P composite coating offers better wear resistance and friction coefficient under higher working temperature conditions due to its higher decomposition temperature (3000 °C) when compared to PTFE (300 °C) [15]. Mohammad Islam experimentally confirms that microhardness of the copper substrate improved to 148% by using the medium phosphorus Ni–P–SiO₂ coating formed at the optimum concentration of SiO₂ (2 g/L). Embedded SiO₂ particles refine the nodular structure and avoiding the porosity of the coating results in an increase in microhardness and corrosion resistance of the Ni–P coating in 4 wt% of NaCl solution for 2–4 weeks [16]. D. Dong found that higher surface area of SiO₂ particles increases the deposition rate of Ni–P–SiO₂ coating compared to Ni–P coating. SiO₂ particles retard the plastic deformation of the Ni matrix, which results in an increase in the microhardness of the Ni–P–SiO₂ coating due to as-deposited condition. Formation of crystalline nickel and nickel phosphide at 400 °C annealing temperature improves the microhardness of the composite coating [17]. M Alishahi reported that higher load transfer capability of CNTs results in the higher microhardness of the Ni–P–CNT coating. Formation of rich phosphorus film in 3.5% NaCl solution avoids the dissolution of Ni atoms at the contact surface, which improves the corrosion resistance [18]. Cheng-Kuo Lee confirms that the corrosion resistance of the Ni–P–TiO₂ coating is decreased due to decrease in phosphorus content by the addition of TiO₂. Addition of CNT increases the phosphorus content, which results in better corrosion resistance of the Ni–P–CNT coating [19]. J. N. Balaraju confirms that embedding the higher dispersion strengthening effect of Si₃N₄ nanoparticles into the Ni–P lattice improves the hardness of the Ni–P coating by 10%. Phase transmission of the coating at 400 °C results in a 22% improvement in microhardness of the coating [20]. On the basis of literature survey undertaken, it is revealed that very few studies have been reported on electroless Ni–P–SiC composite coatings. Present investigation focuses on the effect of SiC nano particles concentration and post heat treatment process on micro hardness and corrosion resistance of the Ni–P–SiC composite coating on mild steel substrate.

2 Materials and Methods

2.1 Sample Preparation

Mild steel widely used for various engineering applications is considered as a substrate material with dimensions 15 mm × 15 mm × 2.5 mm. The substrate material is mechanically polished with different grades (100,220,320,420) of SiC grid papers to achieve the same average surface roughness. The substrate is decreased

in the soap solution and activated in 10% HCl solution before submerging into the electroless bath. The substrate is rinsed with distilled water after every step of the pretreatment process. The substrate is immersed in the electroless bath after the pretreatment process. Electroless bath composition and operating conditions are shown in Table 1. To form the composite coating, various amounts of SiC (1–3 g/L) nanoparticles are added to the electroless bath using an ultrasonicator.

2.2 Coating Process

Initially, substrate material dipped into the solution for 90 min to deposit Ni–P alone after that it was shifted to nano-SiC particle-added solution for further 90 min. Solution volume was maintained at 150 ml and indirectly heated with an oil bath and hot plate throughout the coating process. A thermocouple was used to maintain the constant temperature throughout the plating process. Heat treatment process was carried out on the coated substrate at 400 °C for 1 h. Schematic representation of the coating process is shown in Fig. 1.

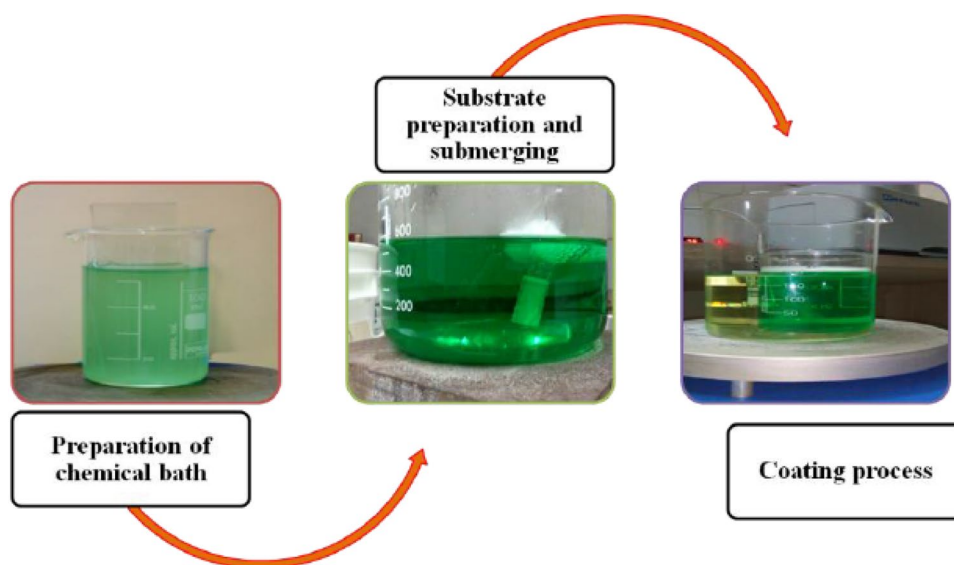
2.3 Analysis of the Coating

Post-heat-treated and deposited conditions of the coating structure was assessed by using X-ray diffraction patterns. Surface morphology and elemental composition of the coating was analyzed by using scanning electron microscope (SEM) with EDX attachment. Coating microhardness was measured by considering the five mean values of indentations at different locations, performed using Vickers hardness tester with a 100 g load and 10 s dwell time. Potentiodynamic polarization technique is used to measure the corrosion resistance of the coating in 3.5% of NaCl solution.

Table 1 Chemical composition and plating parameters

Coating bath composition	Concentration (g/L)
Nickel chloride	40
Sodium hypophosphite	20
Tri sodium citrate	25
Ammonium chloride	50
SDS	0.6
SiC	1–3
Temperature	88 (±2 °C)
pH	4.5–5.5

Fig. 1 Steps followed in the electroless coating



3 Results and Discussions

3.1 XRD Analysis

XRD patterns of Ni–P and Ni–P–SiC coating in as-plated and heat-treated conditions are shown in Fig. 2. XRD pattern confirms that the Ni–P samples show a little amorphous nature with a broad diffraction peak at $2\theta = 44.92$ corresponding to the Ni content. XRD patterns of the post-heat-treated Ni–P coating exhibit three sharp peaks observed at $2\theta = 44.98$, 65.22 , and 82.51 , indicating the crystallization of the coatings, which confirms the phase transmission from amorphous Ni to crystalline Ni₃P. Heat treatment at $400\text{ }^\circ\text{C}$ causes the phosphorus segregation at grain boundaries. Ni atoms present in the matrix reacts with phosphorus, which results in the precipitation of crystalline Ni₃P [21]. More crystalline peaks correspond to the mixed phase of SiC, NiO, and Ni₃P observed in Ni–P–SiC coating. High-intense diffraction peaks corresponding to hexagonal crystalline SiC, FCC NiO, and crystalline Ni₃P are observed in the heat-treated Ni–P–SiC coating. XRD pattern peak intensity confirms the degree of crystallinity, and higher intense peaks mean higher the degree of crystallinity [22].

The diffraction peaks observed at $2\theta = 37.54$, 42.89 , and 79.84 can be indexed to the planes (1 1 1), (2 0 0), and (2 2 2) of (FCC) phase of NiO, respectively, which are well consistent with the standard JCPDS card (47-1049). Crystalline nickel phosphide (Ni₃P) phase peaks at 2θ are acknowledged from JCPDS card 65-2778 as 43.94 , 45.61 , 46.39 , 51.70 , 53.18 , 61.38 , 67.01 , 68.06 , 81.87 , 86.68 , and 90.14 with the planes of (1 1 2), (4 2 0), (2 0 2), (2 2 2), (3 1 2), (3 3 2), (1 6 1), (5 1 2), (7 3 0), (3 4 3), and (2 8 0), respectively. Diffraction peaks identified at $2\theta = 35.6$, 41.5 , 60.06 , 71.78 , and 75.26 can be indexed to the planes (1 1 1), (2 0 0), (2 2 0), (3

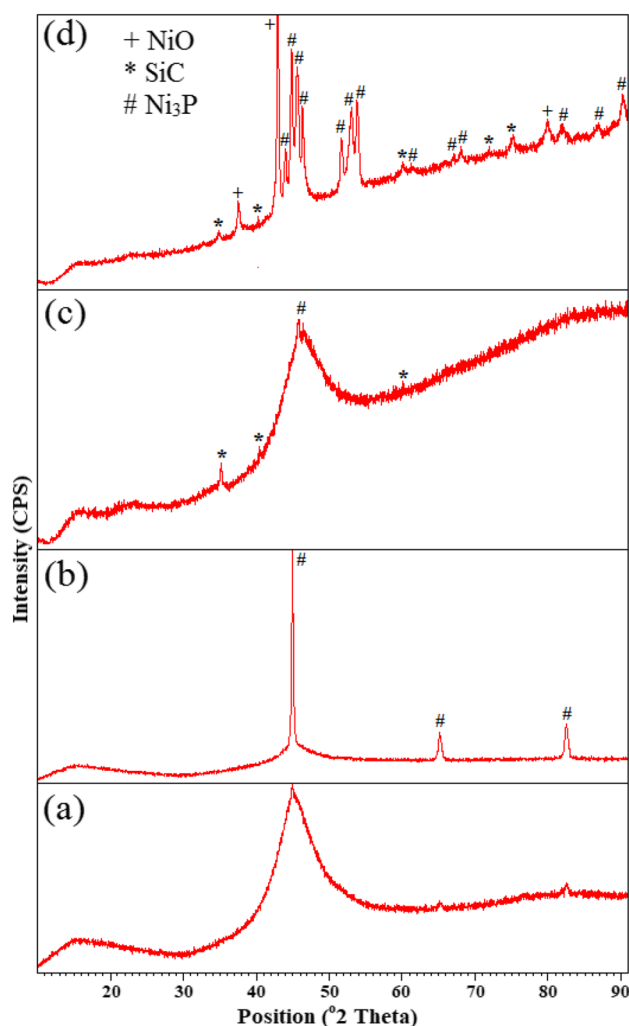


Fig. 2 X-ray diffraction patterns of **a** Ni–P-coated sample **b** Ni–P post heat treated at $400\text{ }^\circ\text{C}$ **c** SiC co-deposited Ni–P as coated **d** Ni–P–SiC post heat treated at $400\text{ }^\circ\text{C}$ for 1 h

1 1), and (2 2 2) of hexagonal crystalline SiC, respectively, and these are acknowledged from JCPDS card 29-1129. Diffraction peaks corresponding to the SiC confirm the co-deposition of SiC nanoparticles with in the Ni–P lattice.

3.2 SEM Analysis

Surface morphology of the electroless Ni–P and Ni–P–SiC coatings formed in the presence of 1 g/L, 2 g/L, and 3 g/L SiC nanoparticles is shown in Fig. 3. The morphological difference between the Ni–P and Ni–P–SiC coating is observed significantly. Reinforcement of SiC refines the grain structure of the Ni–P matrix. Density of co-deposited SiC particles which increases with increasing the particle concentration in the electroless bath results in better surface morphology. Uniform distribution of SiC nanoparticles in the Ni–P lattices is observed up to 2 g/L concentration of SiC beyond this result agglomeration of the particles in the coating. This was confirmed by identifying the

agglomeration sites formed in Ni–P–SiC (3 g/L) coating as shown in Fig. 3d.

3.3 Energy dispersive spectroscopy (EDS) Analysis

Percentage of element composition of Ni–P–SiC coating obtained at various amounts of SiC nanoparticles in the electroless bath is shown in Table 2. Presence of phosphorus and nickel decreases with increasing the SiC concentration.

Table 2 Elemental composition of the composite coatings at various solid contents of SiC nanoparticles

Coating	Ni (wt%)	P (wt%)	Si (wt%)	C (wt%)
Ni–P	87.78	12.22	–	–
Ni–P–SiC(1 g/L)	70.68	8.28	2.73	18.31
Ni–P–SiC(2 g/L)	68.79	7.61	3.69	19.91
Ni–P–SiC(3 g/L)	67.52	6.70	4.50	21.28

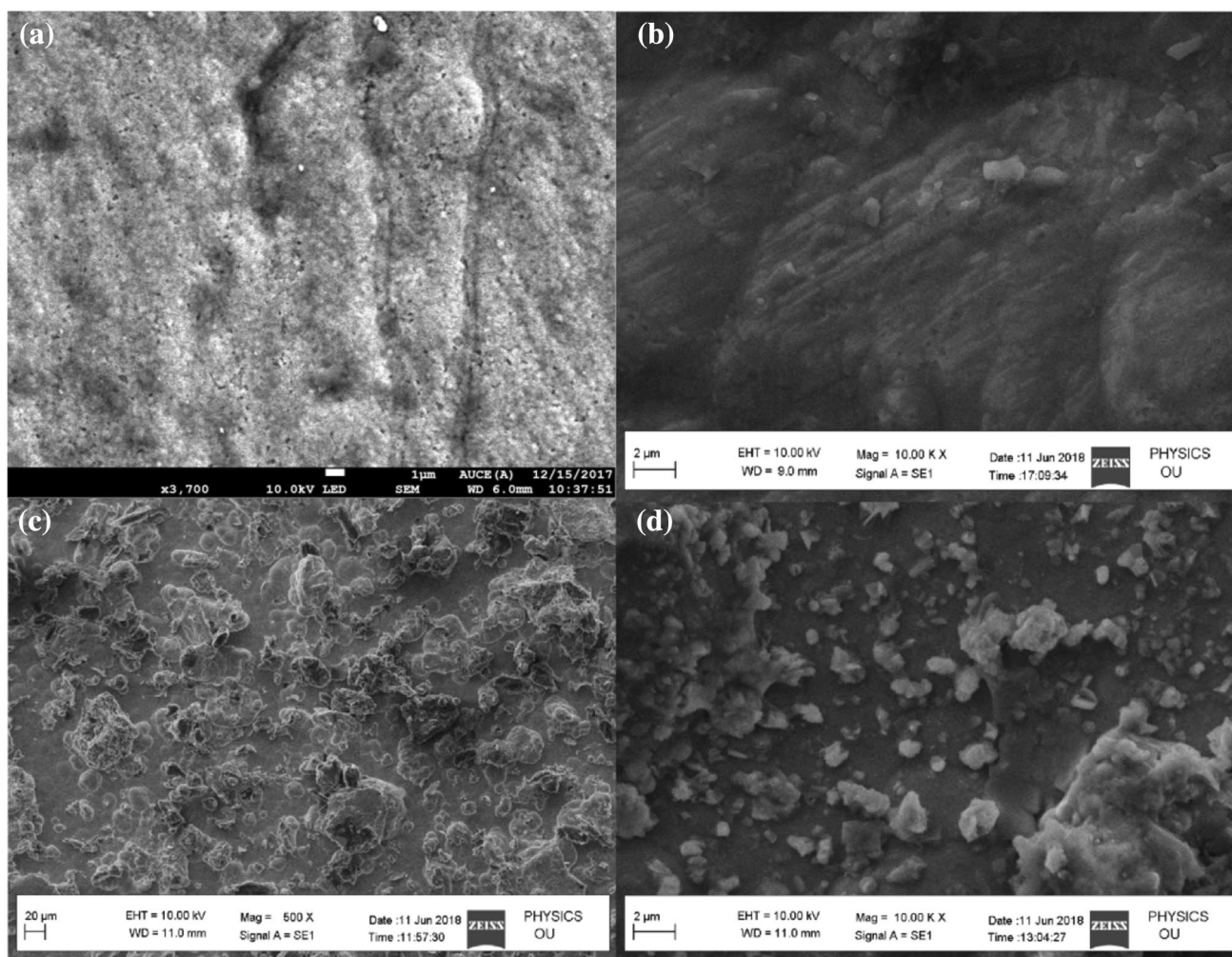


Fig. 3 SEM images of **a** Ni–P coating **b** Ni–P–SiC (1 g/L) coating **c** Ni–P–SiC (2 g/L) coating **d** Ni–P–SiC (3 g/L)

Presence of silicon (Si) and carbon (C) confirms the co-deposition of SiC in the Ni–P matrix. Increase in Si and C percentage confirms the higher deposition of SiC nanoparticles in the coating. Around 6–9 wt% of phosphorus in the Ni–P–SiC coating confirms it is a medium phosphorus coating.

EDS spectra of Ni–P and Ni–P–SiC coating formed at an optimum concentration of SiC (2 g/L) particles are shown in Fig. 4.

3.4 Micro Hardness of the Coating

The surface microhardness of Ni–P and Ni–P–SiC coating formed at various amounts of SiC nanoparticles is shown in Fig. 5. Uniformly distributed embedded hard ceramic nanoparticles with good adhesion to the Ni–P matrix retain the plastic deformation of the matrix, which results in the increase in microhardness of the composite coating [23–25]. Co-deposition of SiC nanoparticles into the Ni–P matrix retains the plastic deformation of the coating which results in increase in microhardness of the Ni–P composite coating. The microhardness of the Ni–P–SiC coating increases, when the SiC nanoparticle concentration in the bath increases from 1 g/L to 2 g/L and 3 g/L. Maximum microhardness value of 713HV is observed in the coating formed at 2 g/L concentration of SiC nanoparticles in the bath. Limited capability of the softer Ni–P matrix to support the particles and increase in distance between the particles due to agglomeration at higher concentration of particles decrease the dispersion hardening effect, which results in the decrease in microhardness of the composite coating [26–28]. Nonuniform distribution and agglomeration of SiC nanoparticles observed in the coating formed at 3 g/L concentration result in decrease in microhardness of the coating. Heat treatment process carried at 400 °C improves the microhardness of the Ni–P and Ni–P–SiC coatings. The phase change from the amorphous structure into the hard crystalline nickel phosphide phase (Ni₃P) at 400 °C annealing temperature enhances the microhardness of the coating [29, 30]. Therefore Ni–P–SiC

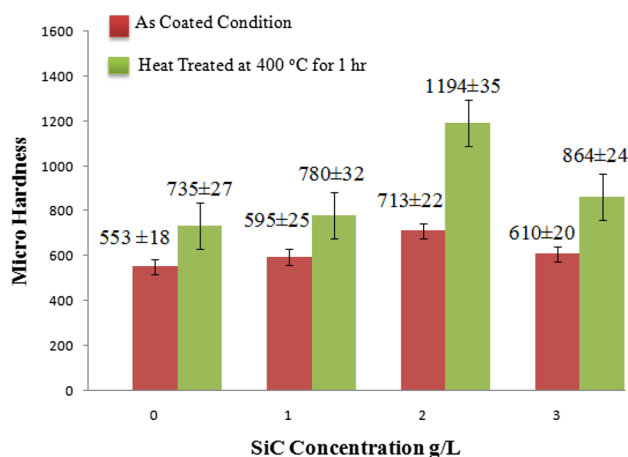


Fig. 5 Micro hardness of the Ni–P and Ni–P–SiC coating in as-coated and heat-treated condition

coating formed at 2 g/L SiC concentration shows the highest microhardness value of 1194HV at 400 °C annealing temperature. The phase change of the coating confirmed by the XRD pattern of the composite coating is shown in Fig. 2.

3.5 Corrosion Behavior of the Composite Coating

As-coated conditions of Ni–P and Ni–P–SiC coatings' potentiodynamic polarization curve in 3.5% NaCl solution are plotted in Fig. 6. Current density (E_{corr}) vs Current potential (i_{corr}) plots are used to characterize the corrosion behavior of the coating. The E_{corr} and the i_{corr} are obtained from cathodic and anodic Tafel curves extrapolation. E_{corr} value of Ni–P coating is shifted to positive direction by the addition of nano-SiC particles in electroless bath which confirms the increasing corrosion resistance of the coating. Lower corrosion current density confirms the lower dissolution rate and higher corrosion resistance of the coating [31–33]. One of the reasons for better corrosion resistance of the Ni–P coating is the formation of hypophosphite film by the oxidation of phosphorus in

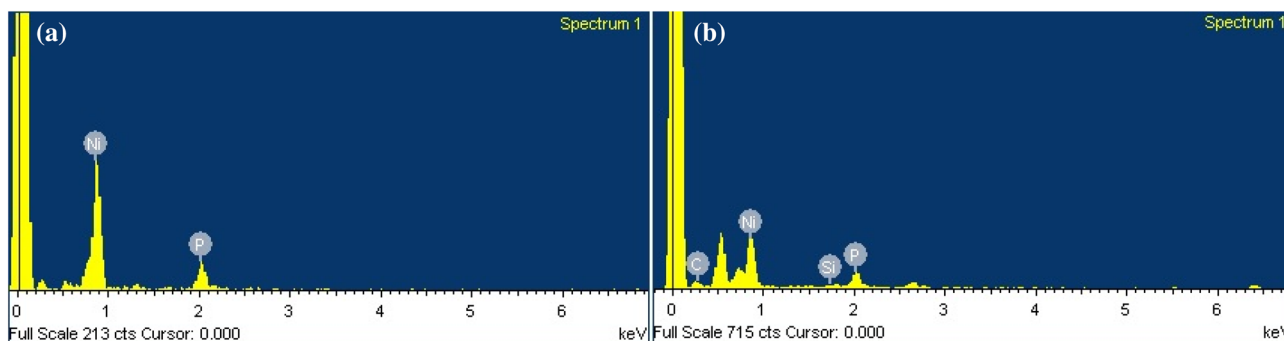


Fig. 4 **a** EDS spectra of Ni–P coating; **b** EDS spectra of Ni–P–SiC coating

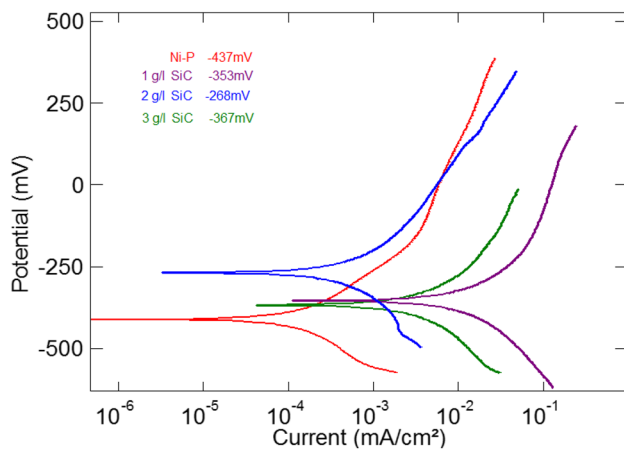


Fig. 6 Polarization curve for Ni–P and Ni–P–ZnO in as-deposited condition

the Ni–P coating, which prevents the interaction of water molecules with Ni, hindering the hydration of nickel [34]. Effect of SiC nanoparticles in the electroless bath on the corrosion resistance of the composite coating is studied by varying the SiC concentration in the bath from 1–3 g/L. Increase in SiC concentration in the bath up to 2 g/L increases the corrosion resistance of the coating due to the uniform distribution of SiC particles in the coating, which fills the pore present in the Ni–P matrix and lowers the metallic area to corrosion [35–37]. Increase beyond 2 g/L SiC concentration in the bath decreases the corrosion resistance of the coating. The coating formed at a higher concentration of SiC (3 g/L) particles in the bath destroys the closed pack structure of the Ni–P lattice which causes the increase in porosity, resulting in the decrease in electrode potential of the coating [38–40]. Therefore, composite coating formed at 3 g/L SiC concentration in the bath shows minimum corrosion resistance.

Corrosion behavior of the Ni–P–SiC coating after heat treatment process is also studied; heat treatment process is carried at 400 °C for 1 h. Corrosion potential and current densities of the composite coating in as-deposited and heat-treated conditions are listed in Table 3. According to polarization curves, shifting of corrosion potential in noble direction after heat treatment process is shown in Fig. 7, which confirms the better corrosion resistance of the post heat-treated Ni–P–SiC coating. Heat treatment process improves the corrosion resistance of the coating due to phase change from an amorphous to crystal structure Ni₃P and development of more corrosion resistance phase [28, 41]. Formation of the Ni₃P and phase transfer from amorphous to crystal structure are confirmed by XRD analysis.

Table 3 E_{corr} and i_{corr} values obtained from the electrochemical polarization curves

Type of coating	As coated		Heat treated at 400 °C for 1 h	
	E_{corr} (mV)	i_{corr} ($\mu\text{A}/\text{cm}^2$)	E_{corr} (mV)	i_{corr} ($\mu\text{A}/\text{cm}^2$)
Ni–P	–437	2.15×10^{-2}	–359	4.16×10^{-3}
Ni–P–SiC (SiC 1 g/L)	–353	7.40×10^{-3}	–317	8.69×10^{-4}
Ni–P–SiC (SiC 2 g/L)	–268	5.55×10^{-3}	–215	1.53×10^{-4}
Ni–P–SiC (SiC 3 g/L)	–367	4.53×10^{-2}	–321	4×10^{-3}

4 Conclusions

Electroless Ni–P and Ni–P–SiC coatings were successfully formed on the mild steel substrate by using sodium hypophosphite, which reduced electroless nickel bath. The detailed experimental procedures discussed and the conclusions of the present work are summarized below.

- Microhardness of the Ni–P–SiC coating improved by increasing the SiC nanoparticles concentration in the electroless bath. The optimal concentration of SiC nanoparticles in the 2 g/L bath was found to obtain maximum microhardness.
- Maximum microhardness of the Ni–P–SiC coating in as-deposited condition is 713HV. The highest microhardness value 1194HV is achieved after heat treatment process due to phase change from amorphous to crystalline nickel and Ni₃P.
- Polarization studies confirm that Ni–P–SiC coating showed better corrosion resistance for mild steel sub-

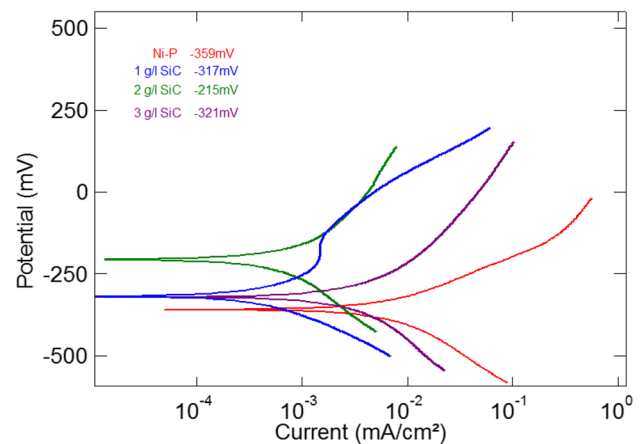


Fig. 7 Polarization curves for Ni–P and Ni–P–SiC post heat-treated condition

strate. SiC concentration in the electroless bath higher than 2 g/L results in a negative effect on the corrosion resistance of the coating.

- Presence of SiC particles in electroless bath up to optimum level perfectly fills the pores present in the Ni–P lattice, which decreases the electrochemically active area of composite coating surface resulting in increase in corrosion resistance. Positive shifting of corrosion potential in noble direction after heat treatment process confirms the increase in corrosion resistance due to phase change. Decrease in microhardness and corrosion resistance is observed in the coating formed at higher concentration of SiC (3 g/L) nanoparticles in the bath due to agglomeration of the nanoparticles.

References

- Balaraju JN, Selvi VE, Rajam KS (2010) Electrochemical behavior of low phosphorus electroless Ni–P–Si₃N₄ composite coatings. *Mater Chem Phys* 120(2–3):546–551
- Sharma S, Sharma S, Agarwala P, Garg R, Gopinath P (2012) A study on Ni–P and Ni–P–ZnO composite coatings developed by electroless technique. *Adv Mater Res* 585:512–516
- Karthikeyan S, Vijayaraghavan L (2016) Investigation of the surface properties of heat treated electroless Ni–P coating. *Trans IMF* 94(5):265–273
- Yan M, Ying HG, Ma TY (2008) Improved microhardness and wear resistance of the as-deposited electroless Ni–P coating. *Surf Coat Technol* 202:5909–5913
- Wu YC, Li GH, Zhang L (2000) Wear resistance of electroless deposited Ni–P and Ni–P/SiC composite coatings on low alloy cast iron. *Surf Eng* 16(6):506–510
- Ping Z, Cheng G, He Y (2010) Mechanically assisted electroless barrel-plating Ni–P coatings deposited on carbon steel. *J Mater Sci Technol* 26:945–950
- Gao Jiaqiang L, Lei Wu, Yating S, Bin, Wenbin Hu (2005) Electroless Ni–P–SiC composite coatings with superfine particles. *Surf Coat Technol* 200(20–21):5836–5842
- Mafi IR, Dehghanian C (2011) Studying the effects of the addition of TiN nanoparticles to Ni–P electroless coatings. *Appl Surf Sci* 258(5):1876–1880
- Ranganatha S, Venkatesha TV, Vathsala K (2010) Development of electroless Ni–Zn–P/nano-TiO₂ composite coatings and their properties. *Appl Surf Sci* 256(24):7377–7383
- Farzaneh A, Mohammadi M, Ehteshamzadeh M, Mohammadi F (2013) Electrochemical and structural properties of electroless Ni–P–SiC nanocomposite coatings. *Appl Surf Sci* 276(1):697–704
- Afroukhteh S, Dehghaniann C, Emamy M (2012) Preparation of electroless Ni–P composite coatings containing nano-scattered alumina in presence of polymeric surfactant. *Prog Nat Sci* 22(4):318–325
- Gawad SAA, Baraka AM, Morsi MS, Eltoun MA (2013) Development of electroless Ni–P–Al₂O₃ and Ni–P–TiO₂ composite coatings from alkaline hypophosphite gluconate baths and their properties. *Int J Electrochem Sci* 8:1722–1734
- Karthikeyan S, Vijayaraghavan L (2015) Effect of co-deposition of Al₂O₃ particle on the properties of electroless Ni–P coating. *Int J Eng Res Technol* 3:175–178
- Lin CJ, Chen KC, He JL (2006) The cavitation erosion behavior of electroless Ni–P–SiC composite coating. *Wear* 261(11–12):1390–1396
- Ploof L (2008) Electroless nickel composite coatings. *Adv Mater Process* 166(5):36–38
- Islam M, Azhar MR, Fredj N et al (2015) Influence of SiO₂ nanoparticles on hardness and corrosion resistance of electroless Ni–P coatings. *Surf Coat Technol* 261:141–148
- Dong XH, Chen WT, Xiao GB, Yang, Zhang PY (2009) Preparation and properties of electroless Ni–P–SiO₂ composite coatings. *Appl Surf Sci* 255:7051–7055
- Alishahi M, Monirvaghefi SM, Saatchi A, Hosseini SM (2012) The effect of carbon nanotubes on the corrosion and tribological behavior of electroless Ni–P–CNT composite coating. *Appl Surf Sci* 258(7):2439–2446
- Lee CK (2012) Comparative corrosion resistance of electroless Ni–P/nano-TiO₂ and Ni–P/nano-CNT composite coatings on 5083 aluminum alloy. *Int J Electrochem Sci* 7:12941–12954
- Balaraju JN, Raja KS (2012) Electroless deposition and characterization of high phosphorus Ni–P–Si₃N₄ composite coatings. *Int J Electrochem Sci* 7:747–761
- Soleimani R, Mahboubi F, Kazemi M, Arman SY (2014) Corrosion and tribological behaviour of electroless Ni–P/nano-SiC composite coating on aluminium 6061. *Surf Eng* 31(9):714–721
- Yaghoobi M, Bostani B, Farshbaf PA, Ahmadi NP (2018) An investigation on preparation and effects of post heat treatment on electroless nanocrystalline Ni–Sn–P coatings. *Trans Indian Inst Metals* 71(2):393–402
- Chen H, Wang Q (2015) Electroless plating of Ni–P–W coatings containing scattered Nb₂O₅ on sintered NdFeB substrate. *Mater Res* 18(5):1089–1096
- Araghi A, Paydar MH (2014) Wear and corrosion characteristics of electroless Ni–W–P–B₄C and Ni–P–B₄C coatings. *Tribol-Mater Surf Interfaces* 8(3):16–24
- Sarika S, Sharma S, Awanish S, Agarwala V (2016) Co-deposition of synthesized ZnO nanoparticles into Ni–P matrix using electroless technique and their corrosion study. *J Mater Eng Perform* 25(10):4383–4393
- Shu X, Wang Y, Liu C, Gao W (2015) Microstructure and properties of Ni–B–TiO₂ nano-composite coatings fabricated by electroless plating. *Mater Technol* 30(1):A41–A45
- Franco M, Sha W, Malinov S, Rajendran R (2013) Phase composition, microstructure and microhardness of electroless nickel composite coating co-deposited with SiC on cast aluminium LM24 alloy substrate. *Surf Coat Technol* 235:755–763
- Ma C, Wu F, Ning Y, Xia F Liu Y (2014) Effect of heat treatment on structures and corrosion characteristics of electroless Ni–P–SiC nanocomposite coatings. *Ceram Int* 40(7):9279–9284
- Balaraju JN Rajam KS (2005) Electroless deposition of Ni–Cu–P, Ni–W–P and Ni–W–Cu–P alloy. *Surf Coat Technol* 195(2–3):154–161,
- Wu X, Mao J, Zhang Z, Che Y (2015) Improving the properties of 211Z Al alloy by enhanced electroless Ni–P–TiO₂ nanocomposite coatings with TiO₂ sol. *Surf Coat Technol* 270:170–174
- Balaraju J, Narayana TS (2001) Evaluation of the corrosion resistance of electroless Ni–P and Ni–P composite coating by electrochemical impedance spectroscopy. *J Solid State Electrochem* 5:334–338
- Zhou YR, Zhang S, Nie LL (2016) Electro deposition and corrosion resistance of Ni–P–TiN composite coating on AZ91D magnesium alloy. *Trans Nonferr Metals Soc China* 26(11):2976–2987

33. Ranganatha S, Venkatesha TV (2012) Studies on the preparation and properties of electroless Ni–W–P alloy coatings and its nano-MoS₂ composite. *Phys Scr* 85(3):035601
34. Hu J, Fang L, Liao X-L, Shi L-T (2017) Influences of different reinforcement particles on performances of electroless composites. *Surf Eng Vol* 33(5):362–368
35. Faraji S, Faraji AH, Noori SR (2014) An investigation on electroless Cu–P composite coatings with micro and nano-SiC particles. *Mater Des* 54:570–575
36. Allahkaram SR, Alivand RF, Bakhsh MS (2013) Corrosion behavior of electroless Ni-P/Ni-P-ZnO coatings. *Iran J Mater Sci Eng* 10(1):10–17
37. Yang Z, Xu H, Li M, Shi Y, Huang Y, Li H (2004) Preparation and properties of Ni/P single-walled carbon nanotubes composite coatings by means of electroless platin. *Thin Solid Films* 466:86–91
38. Gadhari P, Sahoo P (2014) Effect of process parameters on microhardness of Ni–P–Al₂O₃ composite coatings. *Proc Mater Sci* 6:623–632
39. Zhang S, Han K, Cheng L (2008) The effect of SiC particles added in electroless Ni–P plating solution on the properties of composite coatings. *Surf Coat Technol* 202(12):2807–2812
40. Wanga H-L, Liu L-Y, Dou Y et al (2013) Preparation and corrosion resistance of electroless Ni-P/SiC functionally gradient coatings on AZ91D magnesium alloy. *Appl Surf Sci* 286:319–327
41. Chen HJ, Wang LL, Huang WQ, Hao L (2010) Corrosion characteristics of electroless Ni–P Coatings deposited on W–Cu composite. *Corros Eng Sci Technol* 45(3):235–239